

Effect of Specimen Sizes on Flexural Compressive Strength of Concrete

J.K.Kim

Korea Advanced Institute of Science and Technology, Taejon, Korea

S.T.Yi

Korea Power Engineering Company Inc., Kyunggi, Korea

J.H.J.Kim

Sejong University, Seoul, Korea

ABSTRACT: It is important to consider an effect of a member length when estimating the ultimate strength of a concrete flexural member. Also, it is essential to evaluate the effect of neutral-axis depth on flexural compressive strength of beam. However, the experimental data is still insufficient for a proper evaluation. For all types of loading conditions, the trend is that the strength of a member tends to decrease when the member length and depth increase. In this paper, the length and depth variations of a flexural compressive member have been studied experimentally. A series of C-shaped specimens subjected to axial compressive load and bending moment were tested. More specifically, four different length ($h=10, 20, 30$ and 40 cm) and three different depth ($c=5, 10$ and 20 cm) concrete specimens are tested to investigate the size effect of member length h and neutral axis depth c , respectively. The thickness of the specimens was kept constant where the size effect in out-of-plan direction is not considered. The test results are curve fitted using Levenberg-Marquardt's Least Square Method (LSM) to obtain parameters for Modified Size Effect Law (MSEL) by Kim et al.. The analysis results show that the effect of specimen length and depth on ultimate strength was apparent, but their effect on the ultimate strain was negligible. Finally, more general parameters for MSEL are suggested.

1 INTRODUCTION

Most concrete structural members experience combined loading conditions composed of compression, tension, moment, and shear. Especially, in the case of reinforced concrete members, the fundamental idea of concrete resisting compressive stress and steel resisting tensile stress is the basic foundation of reinforced concrete structural design. Fracture mechanics based formulation of size effect theory has not been studied rigorously for compression loaded members. The focus of this study is to further develop and clarify compressive size effect in quasi-brittle materials. In this research, size effect of compression loaded reinforced concrete specimens has been experimentally studied with C-shaped specimens.

It is a well known fact that there is an effect of size differences in nominal strength of specimens made with quasibrittle materials (Bazant 1984, Bazant et al. 1991, Bazant & Xi 1991). More specifically, the nominal strength of laboratory size specimens will differ from that of larger structural members used in construction of real structures. The difference in the nominal strength is a direct consequence of energy release into a finite-size fracture process zone (damaged localized zone). In the early 1980's, it became clear that the size effect on the nominal strength of quasibrittle materials failing af-

ter large stable crack growth is caused principally by energy release (Bazant & Xi 1991) and cannot be explained by Weibull-type statistics of random micro-defects. Ever since, the problem of size effect has received increasing attention (Bazant et al. 1991, Bazant & Xi 1991, Bazant & Chen 1997). Description of such a size effect requires an energy analysis of fracture mechanics type.

Gonnerman (1925) experimentally showed that the ratio of the compressive failure stress to the compressive strength decreases as the specimen size increases. Bazant (1984) derived size effect law (SEL) from the dimensional analysis and similitude arguments for geometrically similar structures of different sizes with initial crack considering the energy balance at crack propagation in concrete.

$$\sigma_N = \frac{P_u}{bD} = \frac{Bf_t'}{\sqrt{1 + \frac{D}{\lambda_o d_a}}} \quad (1)$$

where σ_N = nominal strength; P_u = maximum load; b = thickness of specimen; D = characteristic dimension; f_t' = direct tensile strength of concrete cylinder; d_a = maximum aggregate size; and B and λ_o = empirical constants.

Due to the fracture mechanics-based derivation of size effect law, the past researches have focused more on pure tension and shear loading conditions

rather than compressive loading condition. Only recently, the studies (Cotterell 1972, Bazant & Xiang 1994, Jenq & Shah 1991, Bazant & Xiang 1997) on compressive loading based size effect became a focus of interest among researchers.

Currently, researchers in the field accept the conclusion that the failure of concrete loaded in tension is caused by strain localization resulting in a finite size fracture process zone. In the last few years, many researchers (Hillerborg 1988, Bazant 1989, 1993, Vonk 1992, Van 1992, Rokugo 1992) have started to realize that the strain localization also occurs for concrete specimens loaded in compression. Unlike failure caused by pure tension loading which usually takes place in a relatively narrow localized zone, compressive loading failure occurs within a larger damage zone. The compressive failure shows a similar failure mechanism as tensile failure. In both cases, the failure is caused by the distributed splitting cracks in the direction of member length as the lateral deformation increases during the failure progression. However, the compressive failure mechanism is more complex than tensile failure mechanism. Size effect of compressive failure is not as distinct as in tensile failure, because the formation of microcracks in compressive failure is distributed in a wider region than in tensile failure.

Presently, most design codes for concrete structures do not consider the effect of size. Since quasi-brittle materials such as concrete, rock, ice, ceramic, and composite materials fail by formation of cracks, size effect has to be implemented. In compressive failure of quasibrittle materials, the size effect is quite apparent. Though the behavior of compressive failure has been studied extensively, the failure mechanism and its size effect have been insufficiently studied when compared to tensile failure mechanism. However, endeavoring studies by few researchers have continuously progressed the field (Kim et al. 1998, 1999, 2000, Bazant 1987).

Reinforced concrete beams having different lengths with an equal cross-sectional area are shown in Figure 1a. Reinforced concrete beams having the same length and thickness with different depths are shown in Figure 1b. When evaluating the ultimate strength of a reinforced concrete beam member, the effect of member length is usually not taken into account. In other words, if reinforced concrete beam properties such as compressive strength, longitudinal reinforcement ratio, geometric section dimensions, et cetera are equivalent, flexural strength of the beams with different specimen lengths shall be equal. The effect of neutral-axis depth on flexural compressive strength of beams is also important. However, the experimental data currently available for proper analyses of size effect is lacking at best. From the few available experimental data, it is apparent that the flexural strength decreases as specimen length or depth increase. This phenomenon of

reduction in strength dependent on specimen size is called "Reduction Phenomenon".

For the experiments of concrete beams (Fig. 1) subjected to flexural loads, the length or depth effect can not be evaluated systematically due to the change in the location of neutral axis of the cross section as member sizes, reinforcement ratios, applied loading increments, loading point locations, et cetera vary. To resolve these problems, a series of experiments for C-shaped concrete specimens (Fig. 2) subjected to axial load and bending moment are performed following the test procedure of Hognestad et al. (1955), Kaar et al. (1977), Swartz et al. (1985). The position of neutral axis c is kept fixed by continuously monitoring strains on one surface of the C-shaped specimen and adjusting the eccentricity of the applied force so that the strains on the neutral surface remains zero.

The purpose of this paper is to experimentally investigate the relationship between flexural compressive strength of reinforced concrete beam and its length and depth. For an unreinforced or less than minimal reinforcement required reinforced concrete beam, the beam fails catastrophically in tension as cracks initiate. Therefore, for the beams with this type of failure, size effect is different from beams with reinforcements greater than the minimal required reinforcement in the code. Thus, this study can only be applied to beams which contain a reinforcement ratio more than the minimal required flexural reinforcement defined in the code, but less than the maximum or so-called "75 % of balanced reinforcement".

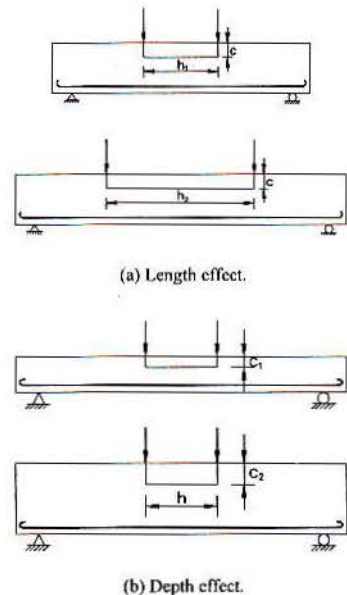


Figure 1. Reinforced concrete beams.

2 TEST SPECIMENS AND EXPERIMENTAL PROCEDURE

2.1 Main test variable

The shape of specimens and the test procedures used were similar to those of Hognestad et al. (1955), Kaar et al. (1977), Swartz et al. (1985). Specimen length : depth ratios of 1:1, 2:1, 3:1, and 4:1 are used to study the effect of length where a constant depth ($c=10$ cm) was maintained and specimen lengths were varied from 10 to 20 to 30 to 40 cm (Fig. 2a).

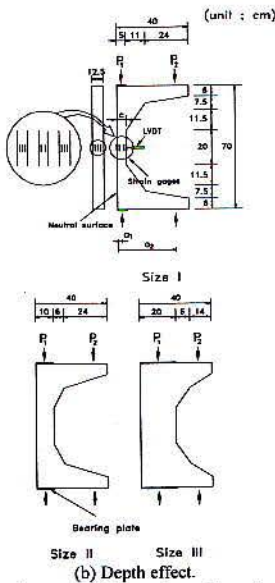
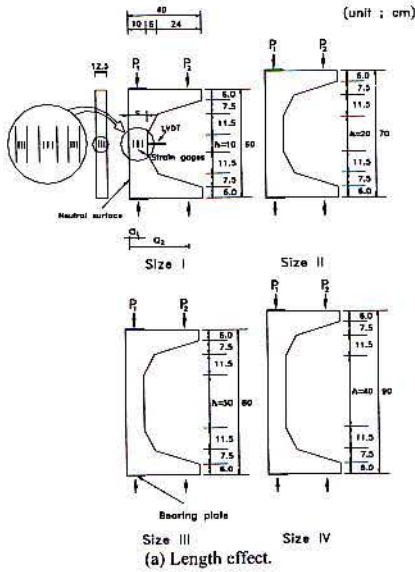


Figure 2. Sizes, shape, and dimensions of specimens.

Specimen length : depth ratios of 1:1, 2:1, and 4:1 are used to study the effect of depth where a constant height ($h=20$ cm) was maintained and specimen depths were varied from 5 to 10 to 20 cm (Fig. 2b). The thickness of all specimens was kept constant ($b=12.5$ cm) to eliminate the out-of-plan size effect. The specimen thickness b is chosen to allow stable failure. The average concrete compressive strengths for the length and depth size effect were 58 and 55 MPa, respectively.

2.2 Mix design

The concrete mix proportions selected for the C-shaped and 28 day compressive strength cylinder specimens are listed in Table 1. Type I Portland cement was used. Maximum aggregate size d_a was 13 mm and superplasticizer and vibrator were used to improve workability and consolidation of concrete.

Table 1. Concrete mix proportions.

w/c	s/a	Unit weight				S.P.**
		W	C	S	G*	
%	%	kg/m ³	kg/m ³	kg/m ³	kg/m ³	%
37	40	178	480	676	1014	1

* maximum aggregate size of 13mm

** super-plasticizer (ratio of cement weight)

All beam specimens and test cylinders were removed from the mold after 24 hours and wet-cured (specimens for length effect) and dry-cured (specimens for depth effect) in a curing room for 28 days until the testing date. Concrete compressive strength f_c' , splitting tensile strength f_{cr} , and elastic modulus E_c were determined based on an averaged result of three identical $\phi 10 \times 20$ cm cylinders from the same batch. Table 2 tabulates the experimental data of f_c' , f_{cr} and E_c of the concrete cylinders where concrete from the same batch was used to cast C-shaped specimens for length and depth size effect tests. It is important to note that the cylinder and C-shaped specimens for length and depth size effect tests were performed approximately 28 days after casting.

Table 2. Physical properties of concrete.

	f_c'	f_{cr}	E_c
	MPa	MPa	MPa
Length effect	58.0	6.0	3.04×10^4
Depth effect	55.0	5.0	3.10×10^4

2.3 Details of test specimens

The dimensions, shape, and loading point locations of C-shaped specimens used in the experiments are shown in Figure 2. The inner vertical thick solid lines of the hollow circle in Figure 2 represent the locations where strain gages are attached to the sides of specimens. Three specimens per specimen size

are prepared, because they are minimum data points required for the data curve fitting. The mid-height of C-shaped specimens which is the critical section under compression was not reinforced. Flexural and shear reinforcements were inserted at both ends of the specimen to eliminate the undesired shear premature failure at the two end sections and enforce failure in the mid-height of the specimen. During testing, strains were measured up to failure at mid-height of specimen by twelve strain gages. Two LVDTs were used to monitor the horizontal displacement at mid-height. This information was used to adjust the load lever arm distances a_1 and a_2 in calculation of bending moments.

2.4 Test procedure

Displacement-controlled load application is used. Strain increments measured on the mid-height of specimen were 50×10^{-6} mm/mm for all sizes in the elastic region. However, near the peak stress and post-peak regions, the strain increments were gradually reduced to enforce a consistent failure in the specimens of equal size. The major axial compressive load P_1 shown in Figure 2 was applied using a universal testing machine (UTM) with capacity of 2500 kN using a displacement control method. The minor load P_2 also shown in Figure 2 was applied using a hand-operated hydraulic jack of 200 kN capacity.

The testing procedure was as follows:

- (1) An increment of load P_1 was applied.
- (2) P_1 was maintained while incrementally applying load P_2 and monitoring the strain value from the attached strain gages on the tension face.
- (3) On reaching zero strain value (on the average), the load P_2 was maintained while P_1 was further increased.
- (4) This procedure was repeated until the specimen failed.

3 ANALYSIS OF TEST RESULTS

3.1 Test results

Test results for length and depth effect are shown in reference 21. Also, the numbering of the specimen (i.e., L-I-1) and experimental data are tabulated in reference 21. The specimens for length and depth effect are assigned with L and D in the specimen names, respectively. Also, the roman numerals I, II, III, IV represent the size of the specimens with I being the smallest and increase accordingly. The arabic numbers 1, 2, 3 are the three specimens tested for each specimen size. P_u , ϵ_{cu} , and δ represent the added load value of P_1 and P_2 , ultimate strain at failure, and

displacement at center of specimens at failure, respectively. The added load value P_u is used to calculate nominal flexural compressive strength at failure σ_N as P_u/bd .

Eleven specimens and eight specimens for length and depth effect were tested successfully where the stable failure occurred in the middle section of specimens in compressive mode with spalling preceding the failure. The failure shapes were similar to the flexural compression failure of beams under two point loading regardless of specimen sizes. It is important to note that the test data of the specimen numbers L-I-3 and D-III-1 are excluded from the data analysis due to undesired failures at two end sections and the rod that applies load P_2 , respectively.

3.2 Length and depth effect of flexural compressive strength

Kim et al. (1989, 1990) proposed MSEL by adding the size independent strength $\sigma_s (= \alpha f'_c)$ to SEL which was originally proposed by Bazant (1987). However, since this study deals with compressive failure mechanism, the failure strength f'_c used in MSEL must be substituted by the compressive strength f'_c in the new model equation for the prediction of compression loaded size effect. As an application of this law, a set of experiments has been performed on C-shaped specimens subjected to flexural compressive force and cylindrical specimens subjected to uniaxial compressive force (Kim et al. 1998, 1999, 2000).

Because the crack distribution of axial compressive specimens is wider than flexural compressive specimens and the strain gradients of both cases are different, the size effect of axial compressive specimens is less visible than in flexural compressive specimens. The shapes of strain gradients are rectangular and triangular distributions for axial and flexural compressive specimens, respectively. In order to show the difference of strain gradients in axial and flexural compressive specimens, the experiments of length and depth effect were performed. Additionally, for the depth effect experiment, we predicted that the specimens with smaller value of c will show a greater strength since cracks will be concentrated in a finite area.

Markeset & Hillerborg (1995), Markeset (1995) experimentally showed that the post-peak energy per unit area is independent of the specimen length when the slenderness is greater than approximately 2.50 for concrete cylinders. Jansen & Shah (1997) also experimentally showed that pre-peak energy per unit cross-sectional area increases proportionally with specimen length and post-peak energy per unit cross-sectional area does not change with specimen length for lengths greater than 20.0 cm in concrete cylin-

ders. In this study, we conclude that flexural compressive strength does not change for specimens having a length greater than 30.0 cm for C-shaped reinforced concrete specimens as shown in Figure 3.

The modified size effect equation proposed by Kim et al. (1989, 1990) was used as the basic equation for the regression analysis of the experimental results of both length and depth size effect. The predicted depth size effect equation was given as

$$\sigma_N(c) = \frac{Bf_c'}{\sqrt{1 + \frac{c}{l_0} \lambda(c)}} + \alpha f_c' \quad (2)$$

where the function $\lambda(c)$ represent the size of fracture process zone with a strain gradient, l_0 is the width of crack band which is empirically known to be related to the maximum aggregate size (e.g., $l_0 = \lambda_0 d_a$ in which λ_0 is an approximate constant between values of 2.0 and 3.0 (Bazant 1984, Kim et al. 1998, 1999, 2000), B and α are empirical constants of MSEL calculated as 0.70 and 0.47 (Kim et al. 2000), respectively. In the regression analyses, λ_0 was chosen as 2.0 where $l_0 = 2.0 \times d_a = 2.0 \times 2.6 = 5.2$ cm.

Due to the microcrack concentration at the failure zone which intensifies the strain gradient, the size effect becomes distinct. More specifically, if the value of c increases, then the strain gradient and size effect decrease. Therefore, it is assumed that the size of c is inversely proportional to the value of $\lambda(c)$. For the case of length dependent size effect, MSEL equation is similar to Equation 2 except that the depth variable c will be replaced by the length variable h where $\lambda(c)$ is then substituted with $\lambda'(h)$.

In order to obtain an analytical equation which predicts the flexural compressive strength of C-shaped specimens for length effect at failure, MSEL is used. Then, Least Square Method (LSM) regression analyses are performed on for the results of the 11 test data for length effect. Equation 3 is obtained from the analyses and the results are graphed and shown in Figure 3.

$$\sigma_N(h) = \frac{0.70f_c'}{\sqrt{1 + \frac{h}{2.6} \left(1.59 \left(\frac{1}{h} \right)^{0.37} \right)}} + 0.47f_c' \quad (h/c \leq 3.0) \quad (3.a)$$

$$\sigma_N(h) = 0.75f_c' \quad (h/c \geq 3.0) \quad (3.b)$$

where nominal flexural compressive strength σ_N and uniaxial compressive strength f_c' are in MPa and length of C-shaped specimen h is in cm. If the ratio of length and depth h/c is greater than or equal to 3.0, then this ratio h/c shall be 3.0.

To develop an equation for depth effect, LSM regression analyses are also performed on the 8 results from the depth effect series. All techniques and notations are same as for length effect. Equation 4 is

obtained from the analyses and the results are graphically shown in Figure 4.

$$\sigma_N(c) = \frac{0.70f_c'}{\sqrt{1 + \frac{c}{2.6} \left(4.17 \left(\frac{1}{c} \right)^{0.53} \right)}} + 0.47f_c' \quad (4)$$

where depth of C-shaped specimen c is in cm. Figure 3 shows the value $\sigma_N(h)/f_c'$ as a function of the length to depth ratio (h/c). And Figure 4 shows the value $\sigma_N(c)/f_c'$ as a function of the depth c . The hollow circular data points and the thick solid line in Figures 3 and 4 represent experimental data and analytical results from Equations 3 and 4, respectively. Figure 3 indicates a strong length dependent size effect. Equation 3 shows a good agreement with the experimental results. For a length-to-depth ratio greater than 3.0, the failure strength approaches a constant value of 0.75. Figure 4 shows a distinct depth dependent size effect when normalized with the compressive strength f_c' . Equation 4 shows a reasonable agreement with the experimental results.

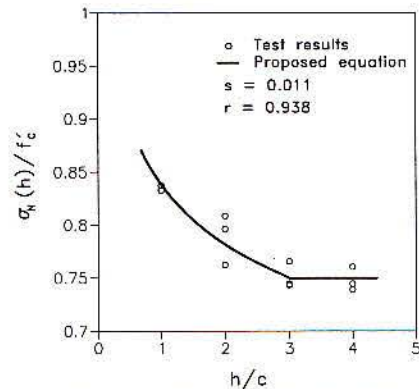


Figure 3. Normalized nominal strength with compressive strength versus ratio of length to depth.

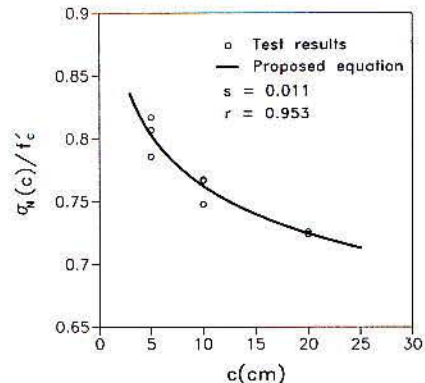


Figure 4. Normalized nominal strength with compressive strength versus depth.

3.3 Generalization of size effect law for C-shaped specimens

Equation 5 was obtained from LSM regression analysis of 19 new experimental data and 20 previous data (Kim et al. 2000) of which the length to depth ratio h/c value was a constant value of 2.0.

$$\sigma_N(c, h) = \frac{0.70 f_c'}{\sqrt{1 + \frac{c}{2.6} \left(0.77 \left(\frac{h}{c} \right)^{0.56} - 0.13 \right)}} + 0.47 f_c' \quad (5)$$

where if $h/c \geq 3.0$, h/c shall be 3.0, and notations are same as in Equations 3 and 4. If the ratio h/c is 2.0, then the value of $\lambda(h/c)$ will be 1.0 and Equation 5 will be same as Equation 1 presented in reference 21 (Kim et al. 2000).

In Figure 5, the thick solid line represents the analytical results obtained using Equation 5 and the hollow circular data points represent the experimental data. The figure shows that Equation 5 agrees with the experimental results quite well. Thus, flexural compressive strength of a beam specimen for various length and depth can be calculated by inputting c , h , and f_c' into Equation 5.

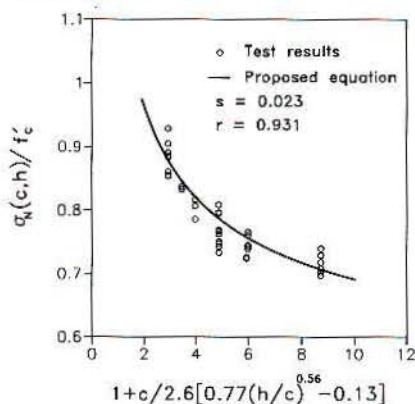
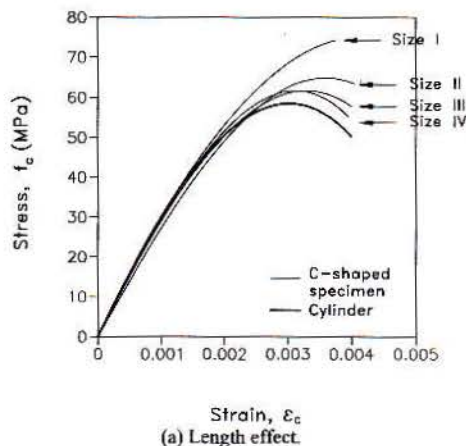


Figure 5. Normalized nominal strength with compressive strength as a function of $1+c/2.6[0.77(h/c)^{0.56}-0.13]$.

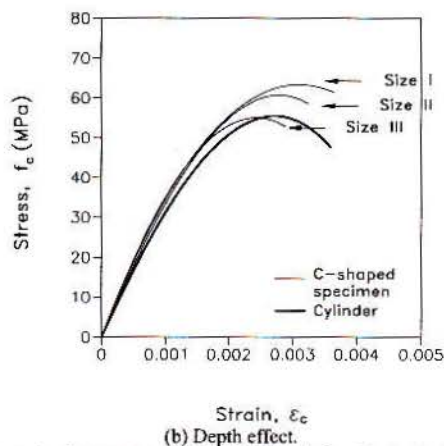
3.4 Stress and strain relationship

Stress values on compressed face f_c obtained from LSM regression analyses using a cubic equation $f_c = A_1 + A_2 \epsilon_c + A_3 \epsilon_c^2 + A_4 \epsilon_c^3$ for length and depth effect of C-shaped specimens are plotted against strain values on compressed face ϵ_c in Figures 6a and 6b, respectively. LSM regression analysis was performed on the data points obtained from the experiments based on satisfying force and moment equilibrium around the neutral-axis of cross-section. In

other words, in order to perform LSM regression, the values of force, moment, and extreme compression fiber strain ϵ_c at every load step are required. LSM regression method minimizes the sum of squares of m nonlinear functions f_i of n -dimensional vector x (column matrix); $\sum f_i^2(x) = \text{Minimum}$. And the coefficients A_1 , A_2 , A_3 , and A_4 are determined. It is assumed that the established f_c and ϵ_c relationship is valid for all layers in the section. Thus, a compressive stress can be determined from this relationship using the measured strain values.



(a) Length effect.



(b) Depth effect.

Figure 6. Comparison of stress-strain relationship in C-shaped specimens and cylinders from experiment.

Also, the thick solid lines in these figures are the uniaxial compressive stress-strain curves obtained from standard concrete cylinder tests. Maximum stress value and the corresponding strain value of C-shaped specimen show a significant increase as the specimen length or depth decreases. For length effect, the maximum stress value and the correspond-

ing strain value of specimen size I is largest when compared to the other specimen sizes.

However, maximum stresses and corresponding strains of C-shaped specimens are relatively similar for specimen sizes III and IV in Figure 6a. The reason for this trend is that flexural compressive strength does not change for specimens having a ratio of length to depth greater than 3.0. For depth size effect, the maximum stress value and the corresponding strain value of specimen size I is largest when compared to the other specimen sizes.

These figures show that there is a brittle failure when concrete with higher strength is used. In order to capture the descending branch of the stress-strain curve, the experiment should be performed using concrete with lower strength. Also, the figures show that stress and strain relationship for concrete in flexural compression may be different from that of a uniaxial compressive strength of cylinders, especially in the descending branch.

3.5 Ultimate strain

It is generally acknowledged that the ultimate strain of concrete ranges between 0.003 and 0.004 based on many experimental results from beams with rectangular cross section subjected to flexural compressive load. Similar results were also obtained in this study for both length and depth size effect cases. In Figure 7, the thick dashed line represents the ultimate strain of 0.003 suggested by ACI Code and the hollow circular data points represent the test results. It was observed that the ultimate strain of every specimen is greater than 0.003 which is similar to the research results reported by Hognestad et al. (1955), Kaar et al. (1977), Nedderman et al. (1973), Corley (1966). Although there is a minute scattering of data points for larger specimens, the difference is insignificant.

4 CONCLUSIONS

A series of compression tests for 19 C-shaped concrete specimens and cylinders cast from the same batch were performed to evaluate the length and depth effects on the flexural compressive strength of flexural members. From the test results and analyses, the following conclusions are drawn.

1. Length effect is apparent (i.e., the flexural compressive strength at failure decreases as the specimen length increases). Depth effect is also distinct. New parameter values of MSEL are suggested which better predicts the "reduction phenomena" of the strength. More general parameter values are also suggested using the previous data (Kim et al. 2000).

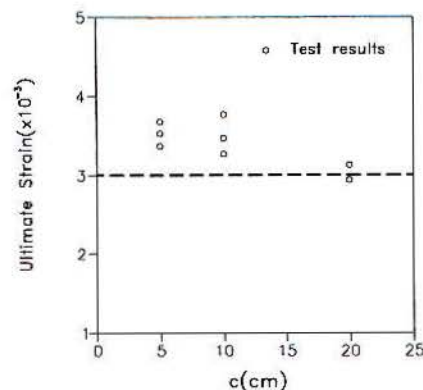
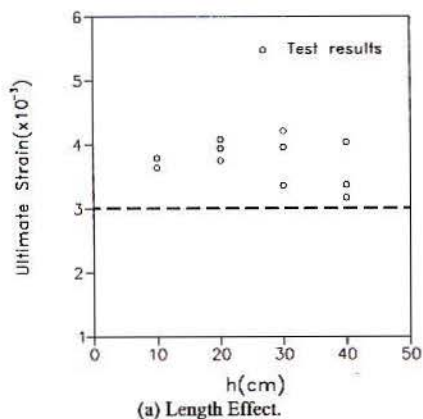


Figure 7. Comparison of ultimate strain with specimen size.

2. For stress and strain relationship, the length and depth effect is also apparent. However, for specimens with a length-to-depth ratio greater than 3.0, length effect of flexural compressive strengths is insignificant. However, it would be desirable in the future to test specimens of broader size ranges.
3. Ultimate strains for both cases range between 0.003 and 0.004. They are similar to general test results for beams and are greater than the value of 0.003 suggested by ACI Code.
4. The results suggest that the current strength criteria based design practice should be reviewed.

REFERENCES

1. Bazant, Z.P. 1987. Fracture Energy of Heterogeneous Materials and Similitude. *SEM-RILEM International Conference on Fracture of Concrete and Rock*: 390-402.
2. Bazant, Z.P. 1989. Identification of Strain-Softening Constitutive Relation from Uniaxial Tests by Series Coupling Model for Localization. *Cement and Concrete Research* 19: 973-977.

3. Bazant, Z.P. 1984. Size Effect in Blunt Fracture; Concrete, Rock, Metal. *J. of Engineering Mechanics-ASCE* 110(4): 518-535.
4. Bazant, Z.P. 1993. Size Effect in Tensile and Compressive Quasibrittle Failures. *Proc. of the JCI Int. Workshop, Size Effect in Concrete Structures, held in Sendai, Japan, (edited by Mihashi H., Okamura, H. and Bazant, Z.P.), E&FN Spon London: 161-180.*
5. Bazant, Z.P. & Chen, E.P. 1997. Scaling of Structural Failure. *Appl. Mech. Reviews-ASME* 50(10): 593-627.
6. Bazant, Z.P. & Xi, Y. 1991. Statistical Size Effect in Quasibrittle Structures: II. Nonlocal Theory. *J. of Engineering Mechanics-ASCE* 117(11): 2623-2640.
7. Bazant, Z.P., Xi, Y. & Reid, S.G. 1991. Statistical Size Effect in Quasi-brittle Structures: I. Is Weibull theory applicable? *J. of Engineering Mechanics-ASCE* 117(11): 2609-2622.
8. Bazant, Z.P. & Xiang, Y. 1994. Compression Failure of Quasibrittle Materials and Size Effect. *AMD Symp. Ser. ASME Appl. Mech. Div., 185, Damage Mechanics in Composites, ASME Winter Annual Meeting. Chicago, Allen, D.H. & Ju, J.W., eds.; 143-148.*
9. Bazant, Z.P. & Xiang, Y. 1997. Size Effect in Compression Fracture: Splitting Crack Band Propagation. *J. of Engineering Mechanics-ASCE* 123(2): 162-172.
10. Corley, G.W. 1966. Rotational Capacity of Reinforced Concrete Beams. *ASCE Proceedings* 92(5): 121-146.
11. Cotterell, B. 1972. Brittle Fracture in Compression. *Int. J. Fracture Mech.* 8(2): 195-208
12. Gonnerman, H.F. 1925. Effect of Size and Shape of Test Specimen on Compressive Strength of Concrete. *Proc. ASTM* 25: 237-250.
13. Hillerborg, A. 1988. Fracture Mechanics Concepts Applied to Moment Capacity and Rotational Capacity of Reinforced Beams. *Proc. Int. Conf. Fracture and Damage Mechanics of Concrete and Rock, Vienna: 233-240.*
14. Hognestad, E., Hanson, N.W. & McHenry, D. 1955. Concrete Stress Distribution in Ultimate Strength Design. *ACI J.* 52(4): 455-479, also PCA Development Bulletin D6.
15. Jansen, D.C. & Shah, S.P. 1997. Effect of Length on Compressive Strain Softening of Concrete. *J. of Engineering Mechanics-ASCE* 123(1): 25-35.
16. Jenq, Y.S. & Shah, S.P. 1991. Features of Mechanics of Quasi-Brittle Crack Propagation in Concrete. *International Journal of Fracture* 51: 103-120.
17. Kaar, P.H., Hanson, N.W. & Capell H.T. 1977. Stress-Strain Characteristics of High-Strength Concrete. *PCA Research and Development Bulletin RD051.01D: 1-10.*
18. Kim, J.K. & Eo, S.H. 1990. Size Effect in Concrete Specimens with Dissimilar Initial Cracks. *Magazine of Concrete Research* 42(153) 233-238.
19. Kim, J.K., Eo, S.H. & Park, H.K. 1989. Size Effect in Concrete Structures without Initial Crack. *Fracture Mechanics: Application to Concrete, SP-118, ACI Detroit: 179-196.*
20. Kim, J.K., Yi, S.T. & Eo, S.H. 1998. Size Effect of Concrete Compressive Strength for the Non-standard Cylindrical Specimens. *FRAMCOS-3, AEDIFICATIO Publishers: 1973-1982.*
21. Kim, J.K., Yi, S.T. & Kim, J.H.J. 2000. Effect of Specimen Sizes on Flexural Compressive Strength of Concrete. *ACI Structural J.*: (accepted).
22. Kim, J.K., Yi, S.T., Park, C.K. & Eo, S.H. 1999. Size Effect on Compressive Strength of Plain and Spirally Reinforced Concrete Cylinders. *ACI Structural J.* 96(1): 88-94.
23. Kim, J.K., Yi, S.T. & Yang, E.I. 2000. Size Effect on Flexural Compressive Strength of Concrete Specimens. *ACI Structural J.* 97(2): 291-296.
24. Markeset, G. 1995. A Compressive Softening Model for Concrete. *Fracture Mechanics of Concrete Structures, (edited by Wittmann F.H.), FRAMCOS-2 AEDIFICATIO Publishers: 435-443.*
25. Markeset, G. & Hillerborg, A. 1995. Softening of Concrete in Compression Localization and Size Effects. *Cement and Concrete Research* 25(4): 702-708.
26. Nedderman, H. 1973. Flexural Stress Distribution in Very High Strength Concrete. *Masters Degree Thesis, Department of Civil Engineering, University of Texas at Arlington.*
27. Rokugo, K. & Koyanagi, W. 1992. Role of Compressive Fracture Energy of Concrete on the Failure Behaviour of Reinforced Concrete Beams. in *Applications of Fracture Mechanics to Reinforced Concrete (ed. A. Carpeneri), Elsevier Applied Science: 437-464.*
28. Swartz, S.E., Nikaen, A., Narayan Babu, H.D., Periyakaruppan, N. & Refai, T.M.E. 1985. Structural Bending Properties of Higher Strength Concrete. *High-Strength Concrete, SP-87, ACI: 147-178.*
29. Van Mier, J.G.M. 1992. Scaling in Tensile and Compressive Fracture of Concrete. in *Applications of Fracture Mechanics to Reinforced Concrete (ed. A. Carpeneri), Elsevier Applied Science: 95-135.*
30. Vonk, R.A. 1992. Softening of Concrete Loaded in Compression. *Ph. D. thesis Eindhoven University of Technology, the Netherlands.*